Advances in Science and Technology Research Journal

Advances in Science and Technology Research Journal, 2025, 19(10), 436–443
https://doi.org/10.12913/22998624/207623
ISSN 2299-8624, License CC-BY 4.0

Received: 2025.06.13
Accepted: 2025.08.15
Published: 2025.09.01

Error metrics in modeling and optimization of the straight-core lossy mode resonance-based sensors

Michał Szymański[1*], Marcin Bator[1], Krzysztof Gajowniczek[1]

[1] Institute of Information Technology, Warsaw University of Life Sciences-SGGW, ul. Nowoursynowska 159, 02-776 Warszawa, Poland
* Corresponding author's e-mail: michal_szymanski@sggw.edu.pl

ABSTRACT

A proprietary open-source simulation and optimization framework, named lossy mode resonance (LMR), was used to model sensors with cylindrical geometry. Particular attention was given to the analysis of two fitness functions used in parameter optimization: the commonly applied mean squared error (MSE) and a custom-designed metric, the valley error (VE). The VE metric was demonstrated to be more suitable for capturing spectral features essential to LMR sensor performance, such as the position and shape of the resonance dip. Simulation studies involving TiO_2-based coatings with varying thicknesses highlight the practical advantages of using the VE metric, especially in the cases where a precise determination of the refractive index and the extinction coefficient is required without prior knowledge of the layer thickness. Compared to MSE, VE provides more accurate and functionally relevant optimization results. These findings indicate that LMR sensors, when combined with appropriately selected optimization criteria, can serve not only as sensing devices, but also as effective tools for material characterization, offering a potential alternative to ellipsometry. Furthermore, the results reveal that similar spectral responses can be achieved using geometrically distinct sensor designs, suggesting new opportunities for performance tuning through structural optimization.

Keywords: lossy mode resonance, R software, optimization, full search.

INTRODUCTION

Lossy mode resonance (LMR) sensors based on coated optical fibers have emerged as a promising platform for highly sensitive and selective detection in various chemical and biological applications. Advances in thin-film deposition techniques have enabled the fabrication of nanometric coatings with controlled thickness, significantly enhancing the performance of such sensors [1]. However, the development and prototyping of LMR devices remain both expensive and time-consuming, limiting their broader adoption. To overcome these limitations, simulation-based approaches have gained increasing attention as a cost-effective alternative to experimental prototyping [2, 3].

Optical fiber sensors based on resonance phenomena have attracted considerable interest since the 1980s because of their sensitivity and versatility. Among the most studied mechanisms are surface plasmon resonance (SPR) [4] and, introduced about a decade later, lossy mode resonance [5, 6]. While SPR sensors have found widespread use, LMR sensors offer several unique advantages, including the possibility of using a wider range of coating materials and compatibility with both polarizations of light.

In recent years, experimental efforts have increasingly focused on identifying novel coating materials—often complex nanocomposites—for use in LMR-based platforms [7–9]. However, such materials frequently exhibit unknown or poorly characterized optical properties, making

analytical or empirical determination of reflectance parameters difficult. In this context, accurate modeling and numerical simulation of the optical response become essential for both sensor design and material characterization. To address these challenges, several computational tools have been developed [10–12], with varying degrees of flexibility and accessibility.

In author's recent work [3], a free and open-source software framework for LMR simulation and optimization was introduced, initially developed in MATLAB and subsequently reimplemented in the R environment. This platform, referred to as LMR, incorporates a graphical interface as well as supports customization of sensor geometry and materials, thereby providing an accessible tool for researchers and practitioners.

The present study was built on this framework to explore the influence of fitness function design on the optimization of straight-core LMR sensors with cylindrical geometry. Specifically, the widely used mean squared error (MSE) metric was compared with a novel criterion, valley error (VE), which is tailored to capture key spectral features such as the position and shape of the resonance dip. Using TiO_2 coatings of varying thicknesses as a case study, it was demonstrated that the VE metric offers superior performance in scenarios where layer thickness is unknown, but precise determination of refractive index and extinction coefficient is required. This capability positions LMR sensors as potential low-cost alternatives to ellipsometry for material characterization.

The remainder of this paper is organized as follows: Section 2 describes the theoretical model and numerical implementation used for LMR simulation, including a detailed definition of the MSE and VE metrics. Section 3 outlines the simulation parameters. Section 4 presents the results of comparative optimization experiments. Finally, Section 5 discusses the implications of the findings and potential future directions.

LMR MODELING

The mathematical framework used for modeling the LMR sensor response relies primarily on geometrical optics, supplemented by classical electromagnetism to account for light reflection at material boundaries. A crucial quantity of interest is the wavelength-dependent transmitted power $T(\lambda)$ through the modified optical fiber. The system is characterized by the following parameters: D denotes the fiber core diameter, L is the length of the sensing region, α represents the skewness angle of light rays, and θ is the angle between a ray and the local surface normal. The free-space wavenumber is defined as $k_0 = 2\pi/\lambda$, where λ is the wavelength. For clarity, a schematic representation of these parameters is provided in Figure 1.

Power transmission through the sensor

When a beam enters the modified fiber structure, it excites both meridional and skew rays, with mixed transverse electric (TE) and transverse magnetic (TM) polarization components. As the rays propagate, they undergo multiple reflections at the interface between the fiber core and the deposited coating. To describe the transmission

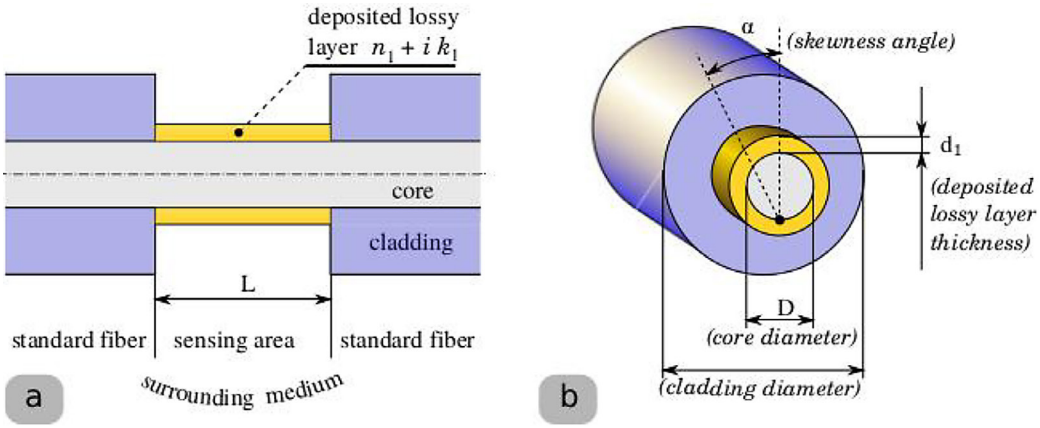

Figure 1. Illustrative drawing of a modified optical fiber [3]. In this paper, the considerations were limited to a single layer deposited on the core and described by a complex refractive index $\tilde{n} = n_1 + ik_1$. (a) the meridional cross section, (b) the transverse cross-section

quantitatively, the reflection coefficient for a single reflection is averaged over both polarizations:

$$R^{N(\theta,\alpha)}(\theta,\lambda) = \frac{R_{TE}^{N(\theta,\alpha)} + R_{TM}^{N(\theta,\alpha)}}{2} \quad (1)$$

where: $N(\theta, \alpha)$ denotes the approximate number of reflections along the sensing area and is given by:

$$N(\theta,\alpha) = \frac{L}{Dtan\theta cos\alpha} \quad (2)$$

Consequently, the normalized transmitted power can be expressed as [10, 11]:

$$T(\lambda) = \frac{\int_0^{\alpha_{max}} \int_{\theta_{cr}}^{\pi/2} R^{N(\theta,\alpha)}\, k_0^2 n_c^2 sin\theta cos\theta \; d\theta \; d\alpha}{\int_0^{\alpha_{max}} \int_{\theta_{cr}}^{\pi/2} k_0^2\, n_c^2 sin\theta cos\theta \; d\theta \; d\alpha} \quad (3)$$

where: n_c is the refractive index of the fiber core and $\theta_{cr} = \arcsin(n_{clad}/n_c)$ is the critical angle determined by the refractive indices of the core and cladding.

Calculation of reflection coefficients and integrals

The reflection coefficients R_{TE} and R_{TM} are calculated using the transfer matrix method, a standard approach for modeling multilayer optical structures. This method relates the tangential components of the electromagnetic fields at the first and last interfaces of the layered stack. In brief, the total transfer matrix M is the product of individual matrices corresponding to each layer. Once M is determined, the reflection coefficients can be extracted and used to evaluate the transmission $T(\lambda)$. Full details of this procedure can be found in [3, 13]. To calculate $T(\lambda)$ the numerator and denominator are calculated separately. The numerator is calculated as numerical integrals (two summing loops), while the denominator is calculated using an equation for solving the integrals analytically. Thus:

$$T(\lambda) = \frac{a(k_0, n_c, \alpha_{max}, \theta_{cr})}{b(k_0, n_c, \alpha_{max}, \theta_{cr})} \quad (4)$$

where:

$$a(k_0, n_c, \alpha_{max}, \theta_{cr}) = \\ = \sum_0^{\alpha_{max}} \sum_{\theta_{cr}}^{\pi/2} R^{N(\theta,\alpha)} k_0^2 n_c^2 sin\theta cos\theta \Delta\theta \Delta\alpha \quad (5)$$

and

$$b(k_0, n_c, \alpha_{max}, \theta_{cr}) = \\ = \frac{1}{4}(n_c k_0)^2 \alpha_{max}(1 + cos2\theta_{cr}) \quad (6)$$

Fitness functions

One of the most commonly used error measures, and often the measure of first choice, is the mean squared error:

$$MSE = \frac{1}{n}\sum_{i=1}^{n}(t_i - o_i)^2 \quad (7)$$

where: t_i and o_i stand for the original and optimized transmission, respectively, and i is index of sequent λ.

For this reason, *MSE* was also implemented in the *LMR* program. However, later simulations showed some shortcomings of this approach. This issue was discussed in detail in the "Results and Discussion" section. Here, however, another measure was proposed, which was called the Valley Error. Its essence can be explained using the illustrative Figure 2, where five points are marked on each function. Two represent the limit values on the x axis, one is the global minimum of the function, and the last two points represent two maxima, one to the left and one to the right of the minimum of the function. It should be noted that both axes are normalized using the values of the target function. Therefore, the value of the evaluated function can have values outside the range of 0–1. The next step is to sum the distances of corresponding points (for both axes) on the target graph and evaluated graphs. The Manhattan metric was taken to express the distance between the points, due to its computational simplicity. Thus:

$$VE = \sum_{i=1}^{5} d\,(o_i, t_i) \quad (8)$$

where: $d(,)$ is a distance (here it is the manhattan one), and $i \in \{1, 2, 3, 4, 5\}$ respectively: 1 – the first point (on the left), 2 – the last (the first on the right), 3 – global minimum, 4 – maximum on the left form the point number 3, 5 – maximum on the right from the point number 3. If there is more than one point of the same value, the closer point to number 3 is taken.

SIMULATION

As outlined in the Introduction, the design and analysis of LMR-based optical fiber sensors increasingly rely on numerical methods due to the high cost and complexity of experimental prototyping. This is particularly relevant when

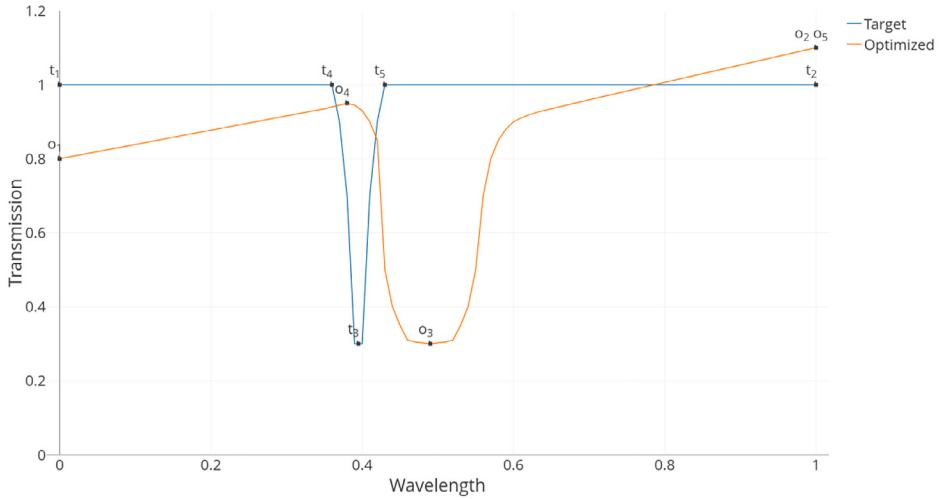

Figure 2. Examples of two functions, where the points used to calculate VE are marked. t_i'*s* lay on the function named target, o_i'*s* – on the function named optimized, while i ∈ {1, 2, 3, 4, 5}

such sensors are considered not only as detection platforms but also as potential tools for material characterization. In such applications, the retrieval of optical constants (n, k) from the transmission spectrum—especially under uncertainty with respect to layer thickness—poses significant modeling and optimization challenges.

To address these issues, a simulation framework was used to evaluate the effectiveness of two distinct fitness functions in optimizing LMR sensor parameters. The first is the widely used MSE, while the second, VE, is a custom-designed metric tailored to capture key spectral features, such as the position and shape of the resonance dip. The simulations were carried out using the proprietary open-source platform LMR [3], which supports flexible geometry and material configuration. The following sections describe the specific simulation scenarios, parameter ranges, and target structures used to validate and compare the performance of both optimization strategies.

Defining a suitable fitness function is typically a nontrivial task, especially in the context of global optimization of LMR-based sensors. The goal is often to find such values of geometric and material parameters that the resulting transmission spectrum exhibits clear, deep, and narrow minima—typically one or more—which are sensitive to changes in the surrounding medium refractive index (SMRI). In this sense, the ultimate objective is to design a highly sensitive sensor.

In this work, the potential of an LMR sensor was further investigated to serve as an alternative to ellipsometry. To the best of authors' knowledge, this is a novel approach that has not been previously reported in the literature. In the considered scenario, the LMR sensor would be used to characterize a material deposited directly on the core in the sensing region. Under ideal deposition conditions, it is assumed that the thickness of the layer is known precisely. However, this assumption may not always hold. Thus, when both the refractive index n and extinction coefficient k of the deposited layer are to be determined from the transmission spectrum—without certainty regarding its thickness—the demands on the fitness function increase considerably.

To explore these challenges, two fitness functions were evaluated: the conventional MSE and a custom-designed metric, VE, introduced earlier in this paper. The validation involved a well-characterized LMR sensor based on a TiO_2 coating, for which both theoretical and experimental results are available in [14]. Two thickness configurations were considered: 333 nm and 1165 nm. Using the proprietary LMR simulation tool described in [3], a full optimization process was performed separately for the MSE and the VE metric. Its aim was to check the optimization process in the case of changing the thickness of the optical fiber.

In the first variant of the sensor test, the objective function was calculated for a device characterized by parameters D = 200 μm, L = 2.5 cm and d = 333 nm. In the search for results, the following optical fiber diameters were used D ∈ {8, 50, 63, 100} μm. Moreover, L ∈ {1, 1.5, 2, 2.5, 3} cm and d was swept in the range [313, 353] nm in 1 nm increments. The waveguide with core

D = 200 μ m was intentionally excluded from the search space to prevent the algorithm from converging self-explanatory to the reference solution regardless of the error measure used. The next sensor test variant, with the TiO_2 layer thickness increased to 1165 nm, provided transmission showing 5 minima (unlike the first case with 1 minimum in the investigated range $0.5 < \lambda < 1.5$ μm). The optimization process was repeated for d varying in the range [1145, 1185] nm.

RESULTS AND DISCUSSION

Ranking of solutions

Throughout this section, the solution indices (e.g., #1, #41, #42) refer to the rankings generated by the employed open-source LMR optimization software [3]. The software employs global optimization strategies guided by the selected fitness function (either MSE or VE). The solution that offers the closest match to the target transmission is assigned index #1, with higher indices denoting progressively less accurate fits. This ranking enables consistent reference across different combinations of parameters and fitness functions.

Case study: 333 nm coating thickness

The transmission spectrum for the structure with a 333 nm TiO_2 layer and D = 200 μm is presented in Figure 3 as the target function. As it can be seen, in the investigated range $0.5 < \lambda < 1.5$ μm, a single resonance dip is present. The optimization results reveal that VE provides better alignment in dip position and shape compared to MSE. This confirms its suitability for spectral fitting in the cases where transmission minima carry the most meaningful information. Figure 4 illustrates the horizontal misalignment problem that arises when using MSE. The figure shows the transmission curves for the best (solution #1), as well as for solutions #41 and #42. All solutions with indices ≤ 41 correspond to L = 1 cm, whereas solutions $41 < n < 83$ correspond to L = 1.5 cm. Thus, solutions #41 and #42 lie on opposite sides of a discrete jump in L. The transmission curve for solution #42 is abruptly shifted towards shorter wavelengths, indicating a discontinuity in the solution space that ideally should be smooth. This highlights another weakness of MSE—it does not penalize such spectral shifts effectively. Additionally, the deeper minimum observed in solution #42 results from the increased interaction length L: a longer sensing region leads to more internal reflections, increasing overall attenuation and lowering transmission.

Case study: 1165 nm coating thickness

The 1165 nm case exhibits multiple resonance dips. Although the VE function was originally designed for single-minimum characteristics, it proves to be robust even in this more complex

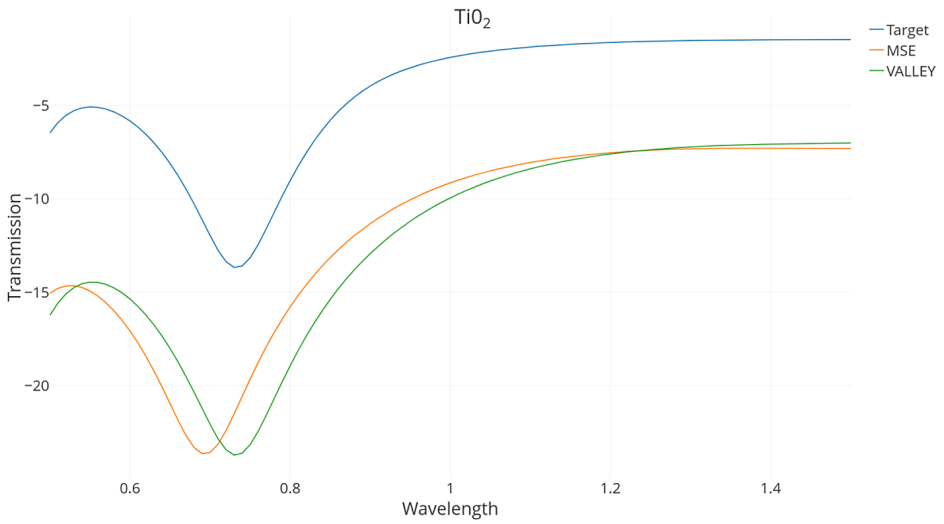

Figure 3. Theoretical analysis of sensor with 333 nm-thick TiO_2 layer. Target function (blue line) is calculated for D = 200 nm and L = 2.5 cm. LMR software, for a fixed value D = 8 μm, provide best-fit solutions for L = 1 cm according to MSE (orange) and VE (green) fitness function

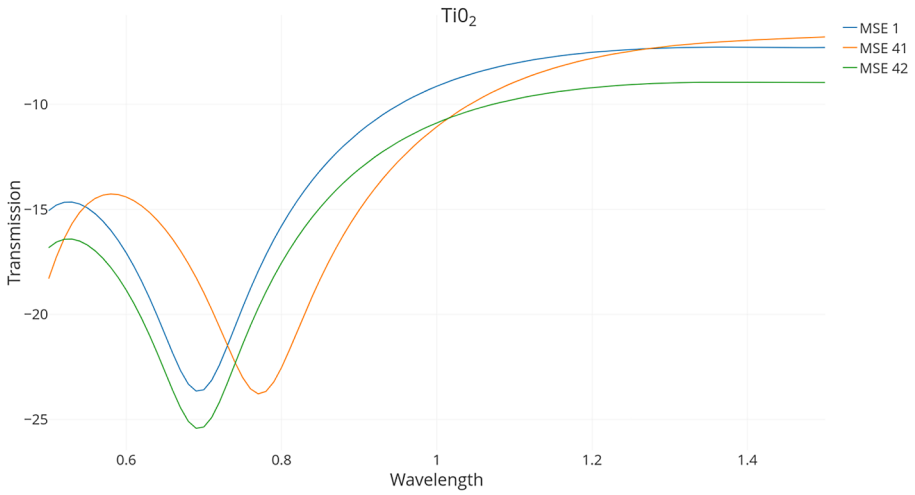

Figure 4. Theoretical analysis of sensor with 333 nm-thick TiO_2 layer. Illustration of the malfunction of the MSE measure, which allows for horizontal shifts of the transmission curve

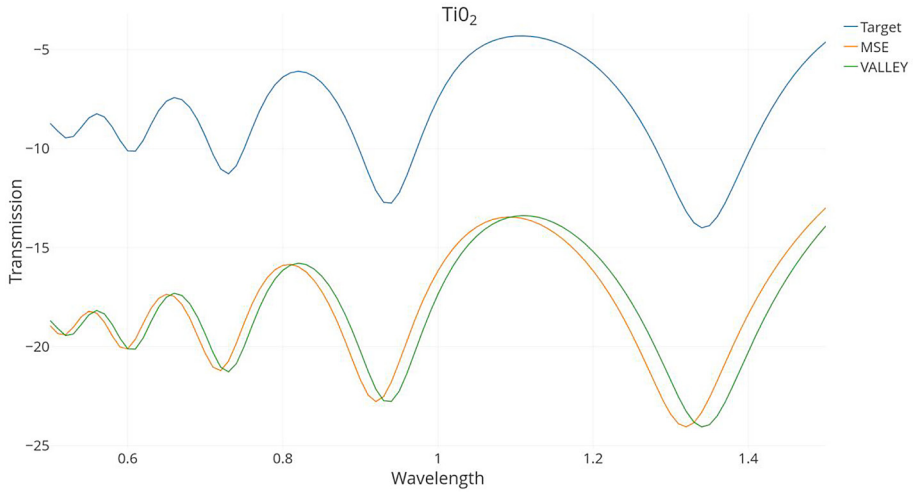

Figure 5. Theoretical analysis of sensor with 1165 nm-thick TiO2 layer. Target function (blue line) is calculated for D = 200 nm and L = 2.5 cm. LM R software, for a fixed value D = 8 μm, provide best-fit solutions for L = 1 cm according to MSE (orange) and VE (green) fitness function

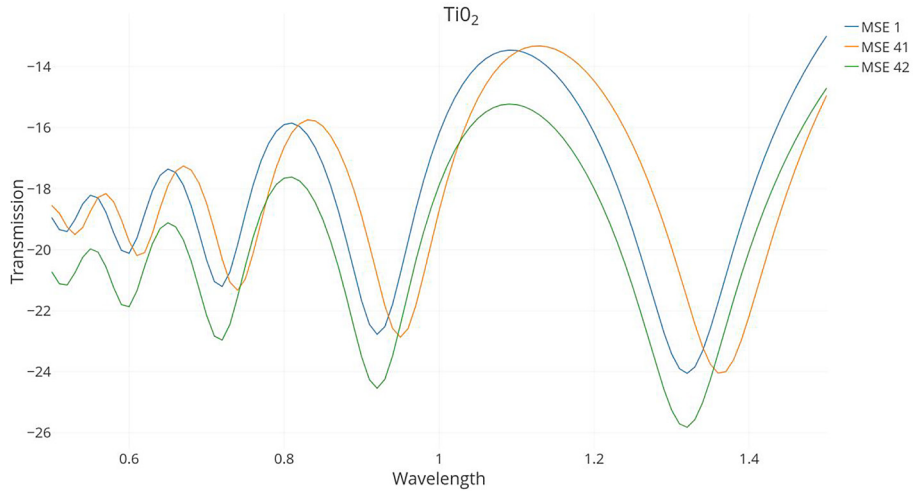

Figure 6. Theoretical analysis of sensor with 1165 nm-thick TiO_2 layer. Illustration of the malfunction of the MSE measure, which allows for horizontal shifts of the transmission curve

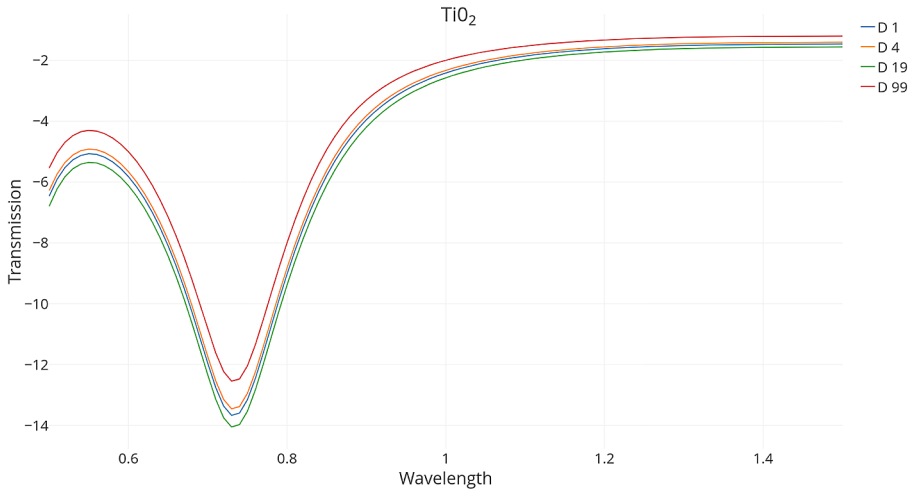

Figure 7. Set of similar transmission curves obtained for a sensor with a 333-nanometer TiO_2 coating layer with different values of D and L parameters

Table 1. Selected solutions for 333-nanometer TiO_2 coating layer leading to similar values of fitness function (FitFun) and the same values λ_{min} = 733 nm

Rank number	*D* [μm]	*L* [cm]	VE FitFun
#1	160	2.0	$7.9*10^{-12}$
#4	210	2.5	0.0164
#19	110	1.5	0.0543
#99	310	3.0	0.4239

scenario. Figure 5 shows the target transmission along with the best fits according to VE and MSE. Again, the horizontal alignment of resonance positions is significantly better for VE, reaffirming its effectiveness. The trends observed in the single-resonance case also appear here. Figure 6 shows analogs of solutions #1, #41, and #42. As in the previous case, the abrupt wavelength shift between solutions #41 and #42 is evident and undesirable. The deeper transmission minimum in solution #42 is again attributed to a longer sensing length (L = 1.5) cm vs. L = 1 cm).

Implications of transmission invariance for sensor design

Interestingly, the study reveals another important insight. An analysis of the solutions generated by the LMR software—both in tabular form (see Table 1) and through graphical representations—demonstrated that it is possible to design multiple sensors with very similar transmission profiles, yet significantly different values of the parameters L and D. An illustrative group of such configurations is presented in Figure 7. This observation is particularly noteworthy in light of study [15], where the authors show that an appropriate selection of L and D can nearly double the sensor's sensitivity.

CONCLUSIONS

This study introduced and validated a novel fitness metric, Valley Error, for the optimization of LMR-based optical fiber sensors. Compared to the widely used Mean Squared Error, the VE metric demonstrated superior capability in preserving critical spectral features, particularly the position and shape of the resonance dip, which are crucial in material characterization tasks. The conducted simulations showed that VE offers better performance in the optimization scenarios where the layer thickness is unknown, enabling more accurate retrieval of refractive index and extinction coefficient values. Additionally, it was observed that MSE tolerates spectral shifts and fails to penalize horizontal misalignments, which may lead to misleadingly high rankings of suboptimal solutions. A secondary yet significant result was the identification of structurally diverse sensor geometries that yield highly similar transmission spectra. This opens up new possibilities for geometry-based tuning of sensor performance without sacrificing spectral fidelity. The findings underscore the importance of using problem-specific error metrics in inverse modeling tasks, especially for the sensors intended as alternatives

to ellipsometry. Future work may explore refining VE to better handle multi-minimum spectra and extending the approach to more complex multi-layer configurations.

REFERENCES

1. Matías IR, Imas JJ, Zamarreño CR. Biosensing based on lossy mode resonances. TrAC Trends Anal Chem. 2024;170:117479
2. Sousa Leal A de, Gonçalves de Paiva IC, dos Passos Rodrigues E, Pereira HA. An open source simulator for prism sensors based on lossy mode resonance effect. Sci Rep. 2025;15(1):1–21
3. Szymański M, Kosiel K, Huk R, Gajowniczek K. LMR: A software for modeling and reverse optimization of straight-core lossy mode resonance (LMR) based sensors. Expert Syst Appl. 2024;251:123925. https://doi.org/10.1016/j.eswa.2024.123925
4. Nylander C, Liedberg B, Lind T. Gas detection by means of surface plasmon resonance. Sens Actuators. 1982; 3:79–88. https://doi.org/10.1016/0250-6874(82)80008-5
5. Marciniak M, Grzegorzewski J, Szustakowski M. Analysis of lossy mode cut-off conditions in planar waveguides with semiconductor guiding layer. IEE Proc J Optoelectron. 1993;140(4):247. https://doi.org/10.1049/ip-j.1993.0040
6. Razansky D, Einziger PD, Adam DR. Broadband absorption spectroscopy via excitation of lossy resonance modes in thin films. Phys Rev Lett. 2005;95(1). https://doi.org/10.1103/physrevlett.95.018101
7. Vikas S, Mishra SK, Mishra AK, Saccomandi P, Verma RK. Recent advances in lossy mode resonance-based fiber optic sensors: A review. Micromachines. 2022;13(11):1921.
8. Hernaez M, Mayes AG, Melendi-Espina S. Sensitivity enhancement of lossy mode resonance-based ethanol sensors by graphene oxide coatings. In: 2017 IEEE Sensors. IEEE; 2017;1–3.
9. Hernaez M, Mayes AG, Melendi-Espina S. Lossy mode resonance generation by graphene oxide coatings onto cladding-removed multimode optical fiber. IEEE Sens J. 2019;19(15):6187–92.
10. Villar ID, Zamarreño CR, Hernaez M, Arregui FJ, Matias IR. Lossy mode resonance generation with indium-tin-oxide-coated optical fibers for sensing applications. J Lightwave Technol. 2010;28(1):111–7. https://doi.org/10.1109/JLT.2009.2036580
11. Paliwal N, John J. Sensitivity enhancement of aluminium doped zinc oxide (AZO) coated lossy mode resonance (LMR) fiber optic sensors using additional layer of oxides. In: Frontiers in Optics 2014. OSA; 2014. https://doi.org/10.1364/fio.2014.jtu3a.40
12. Kosiel K, Koba M, Masiewicz M, Śmietana M. Tailoring properties of lossy-mode resonance optical fiber sensors with atomic layer deposition technique. Opt Laser Technol. 2018;102:213–21. https://doi.org/10.1016/j.optlastec.2018.01.002
13. Chilwell J, Hodgkinson I. Thin-films field-transfer matrix theory of planar multilayer waveguides and reflection from prism-loaded waveguides. J Opt Soc Am A. 1984;1(7):742–53. https://doi.org/10.1364/JOSAA.1.000742
14. Villar ID, Hernaez M, Zamarreño CR, Sánchez P, Fernández-Valdivielso C, Arregui FJ, Matias IR. Design rules for lossy mode resonance based sensors. Appl Opt. 2012;51(19):4298. https://doi.org/10.1364/ao.51.004298
15. Song ZW, Wang Q, Wang XZ. Characterization of the influence of the fiber diameter and sensing region length upon lossy mode resonance (LMR) fiber sensors. Instrum Sci Technol. 2020;48(1):1–21. https://doi.org/10.1080/10739149.2019.1636064